Non-linear Frequency Modulation Using Piecewise Linear Functions for Synthetic Aperture Radar Imaging

Jamal, Saeedi, Amirkabir University of Technology, Electrical Eng. Department, jamal.saeedi@yahoo.com, Iran
Karim, Faez, Amirkabir University of Technology, Electrical Eng. Department, kfaez@aut.ac.ir, Iran

Abstract

In this paper, a new non-linear frequency modulation (NLFM) waveform is developed, which can be used as a transmitted chirp in synthetic aperture radar (SAR) imaging to improve the imaging quality compared to LFM. The new NLFM waveform is constructed based on piecewise linear functions. Time domain signal processing algorithms including time domain correlation and back-projection are investigated in order to use NLFM as the transmitted chirp in SAR system. Strip-map SAR geometry is considered to generate SAR raw signal for point target analysis, in order to validate the new offered waveform.

1 Introduction

Conventional synthetic aperture radar (SAR) systems use linear frequency modulation (LFM) waveform for imaging. Non-linear frequency modulation (NLFM) waveform can be used as an alternative in order to get better SAR imaging quality. In this paper, both the linear and non-linear frequency modulated waveforms are discussed.

Pulse compression is used in radar applications to enhance the range resolution of the radar system without increasing the peak transmitted power [1]. This compression is achieved by modulating the frequency of the transmitted pulse during a pulse width. The most common form of pulse compression waveform is LFM chirp. The matched filter (MF) response of this waveform has a sidelobe level about 13dB, which can be improved by applying many methods like windowing, adaptive filtering [2], and optimization techniques [3]. These techniques can decrease sidelobes level at the cost of reduced signal-to-noise ratio (SNR) and wider mainlobe.

Another pulse compression method is NLFM, which can obtain fine resolution, and good SNR. It has a spectrum weighting function, which results in a pure MF gives low sidelobes. Therefore, the loss in SNR associated with weighting or with the traditional mismatching methods is eliminated [1].

Amplitude tapering of the transmitted signal is an alternative to NLFM for shaping the spectrum. However, this is not practical since efficient power amplification of the waveform requires operating the hardware in a non-linear way. This considerably reduces the ability to maintain accurate amplitude tapering. In addition, this implementation will lead to reduction of transmitted power, and therefore a SNR loss will occur.

By the current progress in developing digital-to-analog converters and large-scale field programmable gate arrays [4], generating accurate digital NLFM waveforms is not still a problem. In this study, we have proposed a new NLFM waveform using piecewise linear (PWL) functions. Compared to the generally used LFM, this chirp is shown to be capable of reducing the sidelobes of MF response without having an adverse effect on SNR and mainlobe width.

The remainder of this paper is organized as follows: Section 2 gives the description of the proposed NLFM waveform. In Section 3, SAR signal processing for NLFM chirp is presented. Section 4 illustrates experimental results. Finally, conclusions are given in Section 5.

2 The Proposed NLFM Waveform

There are many research works to study the NLFM waveforms, and attempt to design the optimum form [5-8]. Generally, there are two NLFM designing procedures. One is based on principle of stationary phase for shaping the spectrum using a window function [5, 7]. The other one is called the explicit functions cluster method, which requires understanding of modulation rules for different NLFM waveforms [9].

The implementation of spectrum shaping may lead to the penalty of mainlobe widening. In other words, there is no control on mainlobe requirement. In this study, NLFM waveform is designed such that its MF response satisfies the sidelobe and mainlobe requirements altogether.

2.1 New NLFM Waveform Using PWL Functions

We propose a method based on generalized PWL functions to generate NLFM waveform. Specifically, instantaneous frequency function is constructed using n-stages PWL functions as shown in **Figure 1**. Most of well-known NLFM waveforms [5-9], have a form of first half reflected, i.e. the second half of the instantaneous frequency is first half reflection. In addition, it is shown through experiments that this kind of transformation leads to a better MF result.

Therefore, first half reflection function is used to generate the second half of the NLFM waveform. The first half of instantaneous frequency of proposed NLFM waveform can be formulated as follows:

$$f(t)=\begin{cases} c_0 t & 0\le t<T_1 \\ B_1+c_1(t-T_1) & T_1\le t<T_2 \\ \dots & \dots \\ B_n+c_n(t-T_n) & T_n\le t<T/2 \end{cases} \tag{1}$$

where B is the frequency bandwidth, T is pulse width, and

$$c_0=\frac{B_1}{T_1},\ \underset{1\le m<n}{\mathrm{c_m}}=\frac{B_{m+1}-B_m}{T_{m+1}-T_m}, c_n=\frac{B/2-B_n}{T/2-T_n}$$

and the second half of NLFM waveform is:

$$f(t)=\begin{cases} B/2\ +c_n(t-T/2) & T/2\le t<T-T_n \\ B-B_n+c_{n-1}(t+T_n-T) & T-T_n\le t<T-T_{n-1} \\ \dots & \dots \\ B-B_1+c_0(t+T_1-T) & T-T_1\le t\le T \end{cases} \tag{2}$$

Then, the phase of this n-stages NLFM waveform can be derived by integrating (1) and (2):

$$\varphi(t)=\begin{cases} c_0t^2/2+l_0 & 0\le t<T_1 \\ B_1t+c_1(t^2/2-T_1t)+l_1 & T_1\le t<T_2 \\ \dots & \dots \\ B_nt+c_n(t^2/2-T_nt)+l_n & T_n\le t<T/2 \end{cases} \tag{3}$$

and the phase function for the second half is:

$$\varphi(t)=$$
$$\begin{cases} t.\frac{B}{2}+c_n\left(\frac{t^2}{2}-t.T/2\right)+h_0 & T/2\le t<T-T_n \\ t.(B-B_n)+c_{n-1}\left(\frac{t^2}{2}+t.(T_n-T)\right)+h_1 & T-T_n\le t<T-T_{n-1} \\ \dots & \dots \\ t.(B-B_1)+c_0\left(\frac{t^2}{2}+t.(T_1-T)\right)+h_n & T-T_1\le t\le T \end{cases} \tag{4}$$

where l_0 … l_n and h_0 … h_n are used to preserve the continuity between different stages of the phase function. Using simple mathematical operations, these parameters are obtained as:

$$l_0=0, l_1=-\frac{1}{2}B_1T_1+\frac{1}{2}c_1T_1^2$$
$$\underset{2\le m\le n}{\mathrm{l_m}}=(B_{m-1}-B_m)T_m+\frac{1}{2}T_m^2(c_{m-1}+c_m)\ -c_{m-1}T_mT_{m-1}+l_{m-1}$$
$$h_0=-\frac{1}{4}BT+\frac{1}{4}c_nT^2+\frac{1}{2}B_nT-\frac{c_nT_nT}{2}+l_n$$
$$h_1=(T-T_n)\left(\left(B_n-\frac{B}{2}\right)+\frac{c_{n-1}}{2}(T-T_n)-\frac{c_nT_n}{2}\right)+h_0$$
$$\underset{2\le m\le n}{\mathrm{h_m}}=(T-T_{n-m+1})\left((B_{n-m+1}-B_{n-m+2})+\frac{c_{n-m+1}}{2}(T-T_{n-m+1})-\frac{c_{n-m+2}}{2}(T_{n-m+1}+T-2T_{n-m+2})\right)+h_{m-1}$$

2.2 Parameters Selection Based on Multi-Objective Optimization

Having the model to generate the phase function for NLFM waveform, there are $2n$ parameters (B_1… B_n, and T_1 … T_n) to be determined to have optimum MF response. The following measures are often used to quantify the performance of MF response: Peak sidelobe level ratio (PSLR), integrated sidelobe level

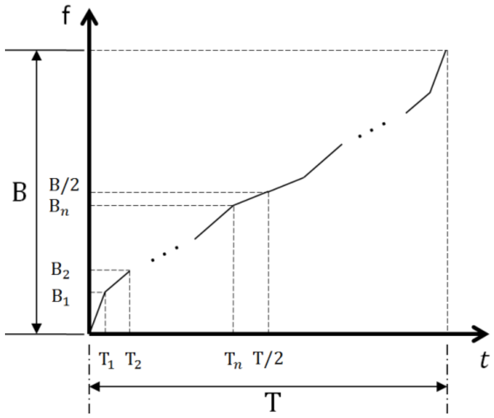

Figure 1: Frequency Modulation signal for n-stages PWL functions.

ratio (ISLR), and 3dB impulse response width (IRW). In order to find the optimum parameters of the new NLFM waveform, a multi-objective optimization should be used to minimize these three objectives simultaneously. To reach this goal we face two challenges. One challenge is to use these three objectives at the same time and the other one is the choice of multi-objective optimizer.

We have chosen goal attainment solver for our multi-objective optimization. Given a set of positive weights w_i, the goal attainment problem tries to find x to minimize the maximum of

$$(F_i(x)-F_i^*)/w_i$$

This minimization is supposed to be accomplished while satisfying all types of constraints including:

$$c(x)\le 0, ceq(x)=0, A.x\le b, Aeq.x=beq, and\ l\le x\le u$$

Here, we have used ISLR and PSLR as two objectives (F_1 and F_2) and IRW is used as a constraint $c(x)<0$, where $c(x)=\mathrm{IRW_x}-v.\mathrm{IRW_{LFM}}$. v is a widening factor that is chosen in order to control the pulse width in the optimization procedure and we set it to 1.35. For getting better ISLR and PSLR, this parameter can be increased. In addition, F_1^* and F_2^* are set to (-40, -65), and the weights are (1, 2), which are obtained through the experiments. Matlab optimization toolbox is used for this purpose.

3 SAR Imaging Using NLFM Waveform

Before the SAR signal is generated, a number of system parameters should be assigned, including carrier frequency, bandwidth, pulse width, and pulse repetition frequency (PRF). The transmitted signal is a NLFM waveform, where the signal spans the bandwidth over the pulse width. This cycle is repeated at the PRF. The SAR signal is usually generated at or near baseband and then mixed up to the desired operating frequency before transmission. The NLFM transmit signal can be expressed as:

$$s_t(t) = A(\mathrm{t})\exp\big(j(2\pi f_0 t + \varphi(t) + \varphi_0)\big) \quad (5)$$

where $A(t)$ is the signal amplitude and defines the pulse length with a rect function, $\varphi(t)$ is the phase function expressed in (3) and (4), f_0 is the frequency at the beginning of the chirp, and φ_0 is the starting phase which can usually be neglected.

In the transmission chain, a power amplifier increases the power to a specified level. A very small portion of the transmit signal is reflected back to the radar. The echoed signal from target can be expressed as

$$s_r(t,\eta) = A'(\mathrm{t})\exp\big(j(2\pi f_0(t-\tau) + \varphi(t-\tau) + \varphi_0)\big) \quad (6)$$

where t is fast time, η is slow time (or azimuth time), and $A'(t)$ is an attenuated version of $A(t)$ and τ is the two-way time of flight to the target at range R.

The received signal is amplified with a low-noise amplifier (LNA) and mixed down to an appropriate band for sampling. After the signal from (6) is mixed down by a frequency, f_m, the signal ready to be recorded is as:

$$s_{rm}(t,\eta) = A''(\mathrm{t})\exp\big(j(2\pi f_0(t-\tau) + \varphi(t-\tau) + \varphi_0 - 2\pi f_m t)\big) \quad (7)$$

For simplification let $f_0 = f_m$, therefore,

$$s_{rm}(t,\eta) = A''(\mathrm{t})\exp\big(j(-2\pi f_0\tau + \varphi(t-\tau) + \varphi_0)\big) \quad (8)$$

SAR systems digitize this data and either store it on board, transmit it to a ground station, or process it on-board.

3.1 Time Domain Correlation

Time-domain correlation (TDC) algorithm uses the raw data directly, without range compression. The platform position for each sample of raw data is used. In this case, SAR image from a point target is formed using the following formula:

$$im(y_0, x_0, z_0) = \textstyle\sum_t \sum_\eta s_{rm}(t,\eta)\exp\left(j\Phi_{\tau_0}(t,\eta)\right) \quad (9)$$

where (y_0, x_0, z_0) is the coordinate of the point target, Φ is the conjugate of the phase in (8), and τ_0 is obtained using the following

$$\tau_0 = \frac{2R(t,\eta)}{c} = \frac{2\sqrt{y_0^2 + z_0^2 + (v(t+\eta) - x_0)^2}}{c} \quad (10)$$

where v is platform velocity and c is light speed.

TDC is a very exact method, but it is very computationally taxing, which is rarely used in practice. However, it is important because it gives a reference for measuring the imaging quality of other reconstruction algorithms.

3.2 Back-Projection

Back-projection (BP) operates on range compressed data [10]. For SAR data, range compression can be performed using MF. Using the start and stop approximation, τ_0 does not depend in fast time t, and we can rewrite (9) as

$$im(y_0, x_0, z_0) = \textstyle\sum_\eta \exp(j2\pi f_0\tau_0)\sum_t s_{rm}(t,\eta)\exp\big(-j\varphi(t-\tau_0)\big) \quad (11)$$

The inner sigma in (11) is the definition of MF. For range compression, we define a reference chirp equal to the transmitted signal. When the received signal is convolved with the reference chirp, the result is a peak where the signals line up. This peak corresponds to the target range. In processing, this is efficiently done with a FFT, a complex phase multiply, and an inverse FFT.

$$s_{rc}(t,\eta) = \textstyle\sum_t s_{rm}(t,\eta)\exp\big(-j\varphi(t-\tau_0)\big) \approx a\,\mathrm{Sinc}\big(\mathrm{b}(t-\tau_0)\big) \quad (12)$$

where a and b are constants. Using (12), (11) can be reformulated as:

$$im(y_0, x_0, z_0) = \textstyle\sum_\eta \exp(j2\pi f_0\tau_0)\, s_{rc}(\tau_0,\eta) \quad (13)$$

The advantages of BP include the simplicity of the algorithm, the parallel computation structure, and the ability to process data from an arbitrary platform path.

4 Experimental Results

In this Section, first we will compare the proposed NLFM waveform with other well-known NFLM waveforms which are designed based on spectrum shaping technique [5-8]. Three different measures including PSLR, ISLR, and IRW are used to quantify the performance of different waveforms.

The simulation parameters are given in **Table 1**, and the simulation results of different waveforms are illustrated in **Table 2**. It can be seen from the results that the proposed NLFM has a better compromise between PSLR, ISLR, and IRW indexes as compared to other alternative waveforms.

In order to validate the new offered chirp signal, strip-map SAR imaging geometry together with different reconstruction algorithms derived in Section 3 are considered. The synthetic example is generated for point target, and it is shown that NLFM chirp can improve imaging quality compared to the LFM waveform. The simulation parameters for SAR system are given in **Table 3**.

After generating the SAR raw signal, RF noise is added to it (RF noise is simulated through filtering the Gaussian noise). It should be mentioned that because of randomness property of noise, RF noise is generated once, and it is used similarly for different experiments.

The results are obtained for three different scenarios including LFM waveform, LFM + windowing and NLFM waveform. Taylor window are typically used in radar applications, such as weighting SAR images and antenna design. Therefore, we have chosen Taylor window for sidelobe reduction of MF response. The parameter of Taylor window is chosen to have an approximately same result compared to NLFM waveform in noise free condition.

The results of point target analysis are shown in **Table 4**. It can be seen that TDC has better performance compared to the BP algorithm. The results for NLFM waveform in both TDC and BP algorithms have shown improvement compared to the LFM waveform and LFM + windowing. Because of the mismatch condition between transmitted and received waveform in LFM + windowing scenario, the SNR is smaller than the NLFM waveform scenario.

For better clarification, reconstructed image contours of TDC and BP algorithms in different scenarios are shown in **Figure 2**. It can be seen from the results that the improvement of using NLFM waveform is clearer for BP algorithm compared to the TDC.

5 Conclusions

In this paper, a new NLFM waveform is proposed, which can be used as a transmitted chirp in SAR imaging to improve the imaging quality compared to LFM. Time domain signal processing algorithms including TDC and BP are modified in order to use NLFM waveform as the transmitted chirp. Experimental results demonstrate effectiveness of the proposed NLFM waveform in terms of SAR image quality metrics. As a future work, modifying the frequency domain algorithms can be considered to process SAR raw signal based on NLFM waveform. Motion compensation techniques can be also investigated for frequency domain algorithms.

Parameter	Value
Pulse width (μs)	13
Bandwidth (MHz)	100
Sampling Frequency (MHz)	360

Table 1: Key simulation parameters.

FM / Index	$PSLR_{dB}$	$ISLR_{dB}$	IRW_{sample}
LFM	-13.38	-4.11	3.54
Cosine, n = 1 [5]	-22.98	-18.71	4.25
Cosine, n = 2	-29.78	-18.00	5.17
Tangent-based [6]	-32.27	-30.04	6.09
Truncated Gaussian [7]	-31.53	-13.47	5.12
Hybrid NLFM [8]	-38.41	-37.58	6.21
Proposed NLFM	-47.36	-37.50	4.81

Table 2: Simulation results of pulse compression of different NLFM waveforms.

Parameter	Value	Parameter	Value
Velocity (m/s)	60	Carier frequency (GHz)	9
Bandwidth (MHz)	100	Sampling frequency (MHz)	220
Pulse width (μs)	35	Flight time (s)	8
Swath width (m)	700	Minimum Range (m)	4663
PRF (Hz)	300	Maximum Range (m)	5361
Altitude (m)	5000	Signal-to-noise ratio (dB)	-45
Incident Angle	45	Azimuth beamwidth (deg)	4

Table 3: SAR system parameters for raw data simulation

Method	Index	$PSLR_{dB}$	$ISLR_{dB}$	IRW_{sample}
TDC (LFM)	Range	-21.88	-10.95	1.12
	Azimuth	-29.61	-12.28	0.73
TDC (LFM+Windoing)	Range	-28.39	-13.32	1.74
	Azimuth	-28.21	-12.54	0.74
TDC (NLFM)	Range	-30.25	-13.31	1.69
	Azimuth	-33.54	-12.58	0.73
BP (LFM)	Range	-15.90	-4.74	1.52
	Azimuth	-20.88	-6.10	0.74
BP (LFM+Windoing)	Range	-27.03	-9.35	1.93
	Azimuth	-21.63	-5.97	0.73
BP (NLFM)	Range	-29.81	-10.24	1.78
	Azimuth	-27.59	-9.27	0.72

Table 4: Results of point target analysis, each sample in azimuth direction is equal to 0.25 m, and in range direction is 1.5 m.

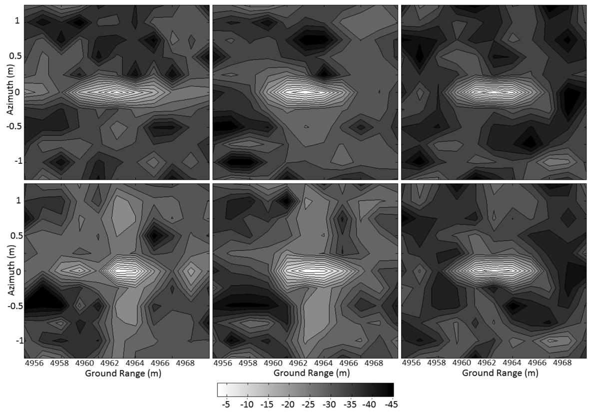

Figure 2: Comparsion of different signal processing algorithms in different scenarios. Top row, left to right: TDC results with LFM, LFM+windowing and NLFM, bottom row: BP algorithm results.

References

[1] M.I. Skolnik, *Radar Handbook 3rd ed*, McGraw-Hill, New York, 2008.

[2] M.H. Ackroyd, and F .Ghani, *Optimum mismatched filters for sidelobe suppression*, IEEE Trans. on Aerospace and Electronic Systems, AES-9, pp.214-218. 1973.

[3] S. R. DeGraaf, *Sidelobe Reduction via Adaptive FIR Filtering in SAR Imagery*, IEEE trans. on image processing, Vol. 3, No. 3, pp.292-301, 1994.

[4] 28Gbps Serial Transceiver Technology White Paper, XILINKS WP385 (v1.1), 2010.

[5] E. Cook, *A Class of Nonlinear FM Pulse Compression Signals*, Proceedings of the IEEE, Vol. 52, No.11, pp.1369-1371, 1964.

[6] N. Levanon, and E. Mozeson, *Radar Signals*, Wiley, Hoboken, New Jersey, 2004.

[7] P.S. Brandon, *The design of a nonlinear pulse compression system to give a low loss high resolution radar performance*, Marconi Rev., 36, pp.1-45. 1973.

[8] R. Price, *Chebyshev low pulse compression sidelobes via a nonlinear FM*, National Radio Science Meeting of URSI, Seattle, WA, 1979.

[9] P. Yichun, P. Shirui, Y. Kefeng, and D. Wenfeng, *Optimization design of nlfm signal and its Pulse compression simulation. Radar Conference*, Proceedings of the IEEE, pp.383 – 386, 2005.

[10] M. Soumekh, *Synthetic Aperture Radar Signal Processing with MATLAB Algorithms*. John Wiley & Sons, Inc., 1999.